Catalytic Mechanism of Fungal Homoserine Transacetylase†

Ishac Nazi and Gerard D. Wright*

Antimicrobial Research Centre, Department of Biochemistry and Biomedical Sciences, McMaster University, Ontario, Canada, L8N 3Z5

Received July 26, 2005; Revised Manuscript Received August 22, 2005

ABSTRACT: Homoserine transacetylase is a required catalyst in the biochemical pathway that metabolizes Asp to Met in fungi. The enzyme from the yeast *Schizosaccharomyces pombe* activates the hydroxyl group of L-homoserine by acetylation from acetyl coenzyme A. This enzyme is unique to fungi and some bacteria and presents an important new target for drug discovery. Steady-state kinetic parameters provide evidence that this enzyme follows a ping-pong mechanism. Proton inventory was consistent with a single-proton transfer, and pH studies suggested the participation of at least one residue with a pK_a value of 6.4−6.6, possibly a His or Asp/Glu in catalysis. Protein sequence alignments indicate that this enzyme belongs to the α/β-hydrolase fold superfamily of enzymes, indicating the involvement of an active-site nucleophile and possibly a canonical catalytic triad. We constructed site-specific mutants and identified Ser163, Asp403, and His432 as the likely active-site residues of a catalytic triad based on steady-state kinetics and genetic complementation of a yeast null mutant. Moreover, unlike the wild-type enzyme, inactive site mutants were not capable of producing an acetyl−enzyme intermediate. Homoserine transacetylase therefore catalyzes the acetylation of L-homoserine via a covalent acyl−enzyme intermediate through an active-site Ser. These results form the basis of future exploitation of this enzyme as an antimicrobial target.

Bacteria, fungi, and plants synthesize the amino acid methionine (Met)[1] from the precursor Asp through a series of enzymatically catalyzed transformations (*1*). These have no parallel in mammals, and as a result, they must acquire this essential amino acid through their diet. Microbes living in nutrient-poor environments must synthesize Met for protein synthesis requirements and as a vital component of the essential biological methyl donor, *S*-adenosylmethionine (SAM) (*2*). In bacteria, the latter is also a precursor to the homoserine lactone class of signaling molecules that can play a role in pathogenesis and biofilm formation (*3*, *4*). Met biosynthesis is therefore an essential microbial process. As a result, this pathway has the potential to be exploited in the control of the growth of microorganisms through the development of specific inhibitors. The antifungal compound 5-hydroxy-4-oxonorvaline, which inhibits the Met biosynthetic enzyme homoserine dehydrogenase, validates this claim (*5*−*7*).

In the first stage of Met biosynthesis, Asp is converted to L-Hse via two successive two-electron-reduction steps. L-Hse can then either be O-phosphorylated, tagging it for processing to Thr, or O-acylated, streaming it for Met biosynthesis. The key acylating enzymes that commit Hse to Met biosynthesis are Hse *O*-acetyltransferase (homoserine transacetylase, HTA) and Hse *O*-succinyltransferase (homoserine transsuccinylase, HTS) (*8*). Both classes of enzymes activate the hydroxyl group of Hse for displacement of the corresponding acid by the thiol of Cys to form cystathionine by the pyridoxal phosphate-dependent enzyme cystathionine γ-synthase. All fungi and many bacterial species such as *Pseudomonas aeruginosa*, *Haemophilus influenzae*, and *Mycobacterium tuberculosis* use HTA, while HTS is found in other bacterial species, e.g., *Escherichia coli* and *Streptococcus pneumoniae*. The HTA and HTS enzymes show no significant primary sequence homology (<10%), but both use covalent catalysis to acylate Hse using their appropriate acylCoAs.

HTAs include two related but distinct families. The bacterial HTAs are roughly 380 amino acids in length, while the fungal enzymes are larger by approximately 100 amino acids (Scheme 1). Both belong to the α/β-hydrolase fold superfamily of enzymes that includes various peptidases, lipases, and esterases (*9*). This family is characterized by an eight-stranded sheet connected by helices. Most adopt an active-site catalytic triad arrangement with the key catalytic amino acids found on loop regions of the proteins. The nucleophilic residue varies, can be Ser, Cys, or Glu, and is found on a structural element termed the nucleophilic elbow. This sharp turn is characterized by the motif Sm-X-Nu-X-Sm-Sm (where Sm is a small residue, e.g., Gly, Nu is the nucleophilic residue, and X is any residue) (*9*). Analysis of

† This research was supported by the Natural Sciences and Engineering Research Council of Canada, Crompton Co./Cie., and by a Canada Research Chair in Antibiotic Biochemistry to G.D.W.

* To whom correspondence should be addressed: Department of Biochemistry and Biomedical Sciences, McMaster University, 1200 Main St. W., Hamilton, Ontario, Canada, L8N 3Z5. Telephone: (905) 525-9140 ext. 22454. Fax: (905) 522-9033. E-mail: wrightge@mcmaster.ca.

[1] Abbreviations: Met, methionine; SAM, *S*-adenosylmethionine; Asp, aspartate; L-Hse, L-homoserine; Thr, threonine; HTA, homoserine transacetylase; HTS, homoserine transsuccinylase; Cys, cysteine; CoA, coenzyme A; HEPES, *N*-(2-hydroxyethyl)piperazine-*N*′-(2-ethanesulfonic acid); DTDP, 4,4′-dithiodipyridine; MES, 2-morpholinoethanesulfonic acid; TAPS, 3-[[tris(hydroxymethyl)methyl]amino]propanesulfonic acid; CHES, *N*-cyclohexyl-2-aminoethanesulfonic acid; SDS, sodium dodecyl sulfate; Tris, tris(hydroxymethyl)aminomethane; EDTA, ethylenediaminetetraacetic acid.

10.1021/bi0514764 CCC: $30.25
Published on Web 09/24/2005

Scheme 1: Schematic Representation of the Difference in the Sequence between the Fungal and Bacterial HTA Amino Acid Sequences

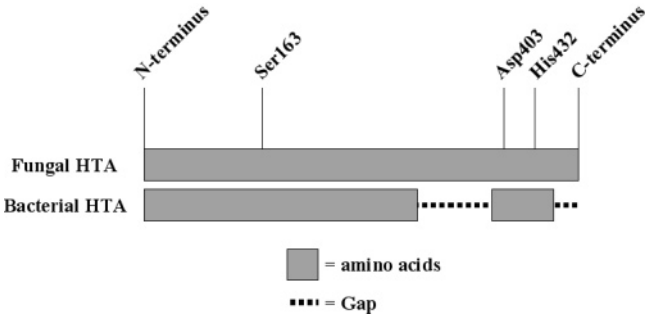

HTAs reveals the conserved motif Gly-Gly-Ser-(Leu/Met/Phe)-Gly-Gly, suggesting that Ser may be a catalytic nucleophilic residue. Born and Blanchard have previously shown that HTA from *H. influenzae* exhibits a ping-pong kinetic mechanism and identifies an acyl−enzyme intermediate by rapid-quench methods (*10*). We report here the first study of a fungal HTA, HTA_{Sp} from the fission yeast *Schizosaccharomyces pombe*, and demonstrate that this class of enzymes uses a covalent catalytic strategy to acetylate homoserine and, using site-directed mutagenesis, identify the likely catalytic triad.

MATERIALS AND METHODS

Cloning, Expression, and Purification of HTA_{Sp}. The predicted *MET2* gene encoding HTA_{Sp} was amplified from *S. pombe* genomic DNA using the oligonucleotides in Table 1 of the Supporting Information. The amplified fragment was cloned into the *Nde* I and *Hind* III restriction enzyme sites of the pET28 vector (Novagen) using standard techniques, and the DNA sequence was verified. The resulting plasmid, pET28 and HTA_{Sp}, was transformed into *E. coli* BL21 (DE3), allowing the expression of HTA_{Sp} with an N-terminal hexahistidine tag.

E. coli BL21 (DE3)/pET28 and HTA_{Sp} was cultured in 2 L of Luria−Bertani broth supplemented with 50 μg/mL kanamycin to an OD_{600} of 0.75 at 37 °C. The cultures were cooled in an ice water bath to 20 °C; isopropyl β-D-thiogalactopyranoside was added to a final concentration of 1 mM, followed by incubation for an additional 2 h at 20 °C in an orbital shaker. The cultures were harvested by centrifugation at 8000*g* for 10 min, resuspended in a final volume of 30 mL of lysis buffer [50 mM HEPES at pH 8.0, 500 mM NaCl, 20 mM imidazole, and 2 complete protease inhibitor cocktail tablets (Roche)], and disrupted by three passes through a French pressure cell at 10 000 psi. Cell debris was removed by centrifugation at 12000*g* for 10 min, and the supernatant was applied onto a 1 mL Ni-NTA agarose column (Qiagen) and washed with 20 mL of buffer A (50 mM HEPES at pH 8.0, 500 mM NaCl, and 20 mM imidazole). A linear gradient of 20−250 mM imidazole in 50 mM HEPES at pH 8.0 and 500 mM NaCl over a period of 25 min was applied, and HTA_{Sp} was eluted between 30 and 50 mM imidazole. Fractions containing recombinant HTA_{Sp} were determined by sodium dodecyl sulfate−polyacrylamide gel electrophoresis.

Steady-State Kinetics. Reaction rates were determined by monitoring the change in absorbance at 324 nm because of the production of CoA by the titration of 4,4′-dithiodipyridine (DTDP $\epsilon_{324\ nm} = 19\,800\ M^{-1}\ cm^{-1}$). Assays were performed in 50 mM HEPES (pH 8.0) containing a varying concentration of up to 3 mM L-Hse, 2 mM DTDP, and a varying concentration of up to 0.2 mM acetylCoA in a final volume of 200 μL. Progress curves were monitored in a Molecular Devices SpectraMAX Plus spectrophotometer using a 96-well flat-bottom polystyrene microtiter plate (VWR). Initial rates were fit to (eq 1) describing Michaelis−Menten kinetics using Grafit 4 software (*11*)

$$v = k_{cat}E_t[S]/(K_m + [S]) \quad (1)$$

Initial rates were also fit to (eq 2) describing the ping-pong Lineweaver−Burk plot in Grafit 4 software (*11*)

$$y = AK_a/V_{max} + (1 + K_b/B)/V_{max} \quad (2)$$

where V_{max} is the maximal velocity, A and B are the concentrations of the substrates, and K_a and K_b are the Michaelis constants for the substrates.

The reactions were performed in 50 mM HEPES (pH 8.0) with an increasing concentration of L-Hse (600, 900, 1200, and 2400 μM) at a fixed concentration of acetylCoA (10, 15, 20, and 40 μM) and monitored via DTDP titration in a final volume of 200 μL.

pH Dependence of the HTA_{Sp} Kinetic Parameters. The activity of HTA_{Sp} was measured at pH 6.5, 7.0, 7.5, 8.0, 8.5, 9.0, and 9.5 to obtain information about the pH dependence of the enzyme-catalyzed reaction. The buffers used for this study were MES (6.5), HEPES (6.5−8.5), TAPS (8.5−9.5), and CHES (9.0−9.5). Assays were performed at room temperature in 50 mM buffer by fixing the concentration of one substrate while varying the other. The pH dependence of the kinetic parameters k_{cat} and k_{cat}/K_m were determined using acetylCoA (5, 10, 15, 20, 25, 50, 125, and 250 μM) and L-Hse (0.1, 0.2, 0.3, 0.4, 0.5, 1.0, 2.5, and 5.0 mM). The data were fit to eqs 3 and 4 using Grafit 4 software (*11*). Equation 3 was used for double-ionization analysis, and eq 4 was used for single ionization analysis.

$$\log v = \log(C/(1 + H/K_a + K_b/H)) \quad (3)$$

$$\log v = \log(C/(1 + K_b/H)) \quad (4)$$

K_a and K_b are respectively the acid and base equilibrium constants; C is the pH-independent value; and H is the proton concentration.

All assays were initiated by the addition of purified HTA_{Sp} (0.15 μg/reaction) and were performed in duplicate.

Proton Inventory Experiments and Solvent Deuterium Isotope Effects. Solvent deuterium isotope effects on k_{cat} and k_{cat}/K_m were determined by using the DTDP assay. The assays were initiated with 0.15 μg/reaction of purified HTA_{Sp}, 25 mM HEPES (pH 8.0), 2 mM DTDP, varying concentrations L-Hse (0.1, 0.2, 0.3, 0.4, 0.5, 1.0, 2.5, and 5.0 mM), and 250 μM acetylCoA, in H_2O or 95% D_2O. The same experiment was performed with varying concentrations of acetylCoA (5, 10, 15, 20, 25, 50, 125, and 250 μM) and 5 mM L-Hse. Proton inventories were determined by measuring the kinetic parameters at varying amounts of D_2O in the

reaction mixture (0, 20, 45, 70, and 95%). Assay conditions were similar to those described for the pH dependence experiment.

Identification of Acetyl−Enzyme Intermediate. The detection of an acetyl−enzyme intermediate was accomplished by monitoring ^{14}C-acetylCoA-dependent labeling of HTA$_{Sp}$. The reaction was initiated with the addition of 10 μg of HTA$_{Sp}$ to ^{14}C-acetylCoA (final concentrations of 200 μM, 50 Ci/mol) in 50 mM HEPES at pH 8.0. The same reaction was performed in the presence of 3 mM L-Hse to chase away the label from the acetyl−enzyme intermediate. The reactions were stopped by the addition of SDS−polyacrylamide gel electrophoresis loading dye (4% SDS, 100 mM Tris at pH 8.8, 50 mM EDTA, 10% glycerol, and 0.02% bromophenol blue) at various time points. These reactions were then applied to a 12% SDS−polyacrylamide gel, dried, and exposed to a Storage Phosphor Screen. The radioactive label was visualized using a Typhoon 9200 Variable Mode Imager and ImageQuant 5.2 software (Molecular Dynamics).

Site-Directed Mutagenesis of HTA$_{Sp}$. To investigate the role of different residues in the mechanism of HTA$_{Sp}$, the site-specific mutants Ser163Ala, Ser163Cys, Asp209Asn, Asp374Asn, Asp403Asn, and His432Ala were prepared using the method of Higuchi et al. (*12*). The oligonucleotides used for the construction of these mutants are outlined in Table 1 of the Supporting Information.

To construct each mutant, two PCR reactions were setup. The first was used to amplify the fragments on either side of the mutation site, and the second was to amplify the entire gene with the site-specific mutation using the PCR fragments from the first amplification as templates. Final PCR products were cloned into the pET28 vector. The expression, purification, and steady-state kinetic analysis of these mutants followed the procedure outlined above for the wild-type enzyme.

Expression of the Site-Specific Mutants in a MET2-Deficient S. cerevisiae. HTA$_{Sp}$, Ser163Ala, Ser163Cys, Asp374Asn, Asp403Asn, and His432Ala mutants were cloned into the pDESTIN vector using the Gateway technology (Invitrogen). These constructs were further used to insert the genes into the pGAL-cflag vector (plasmid MT3164 in ref *13*). Briefly, the genes expressing these enzymes were amplified by PCR using the oligonucleotides 5′-GGGGACAAGTTTGTACAAAAAAGCAGGCTTAATGGAATCTCAATCTCCGATTGAATCA and 5′-GGGGACCACTTTGTACAAGAAAGCTGGGTCCCAGGAGGTTATGTCTTCCATTTCTC. The amplified genes were inserted into the pDONR201 vector as an entry clone. These clones were transformed into TOP10 *E. coli* electrocompetent cells and selected on LB-agar plates supplemented with kanamycin (50 μg/mL). Colonies were screened for the proper insert, and then, the destination clone in the pGAL-cflag vector was also constructed. These constructs were used to transform *Saccharomyces cerevisiae* (ATCC 4011167) (a haploid Met auxotroph that has a *MET2* gene disruption), using the lithium acetate yeast transformation method (*14*).

The *S. cerevisiae* Δ*MET2* Met auxotroph transformed with the wild type and site mutants cloned into the pGAL-cflag expression system were grown in yeast nitrogen base (YNB) broth supplemented with 100 mg/L His, 100 mg/L Lys, 100 mg/L uracil, 2% galactose, and 2% raffinose in the presence or absence of 100 mg/L of Met. Growth of these strains was also tested on similarly supplemented YNB-agar plates.

Table 1: Steady-State Kinetic Parameters of HTA$_{Sp}$ and Site Mutants

enzyme	substrate	K_m (μM)	k_{cat} (s^{-1})	k_{cat}/K_m (s^{-1} M^{-1})
HTA$_{Sp}$	acetylCoA	20.9 ± 1.4	9.34 ± 0.2	4.47×10^5
	L-Hse	1090 ± 80	9.60 ± 0.3	8.83×10^3
	propionylCoA	48.4 ± 3.8	16.1 ± 0.5	3.32×10^5
	butyrylCoA	44.1 ± 3.7	47.2 ± 0.1	1.07×10^5
Ser163Cys	acetylCoA	23.9 ± 3.7	0.64 ± 0.06	2.67×10^4
	L-Hse	6430 ± 340	1.67 ± 0.03	2.61×10^2
Asp209Asn	acetylCoA	19.9 ± 1.7	12.9 ± 0.03	6.50×10^5
	L-Hse	1150 ± 60	8.40 ± 0.03	1.40×10^4
Asp374Asn	acetylCoA	11.6 ± 0.8	8.46 ± 0.1	7.30×10^5
	L-Hse	960.0 ± 50	13.4 ± 0.2	1.40×10^4

RESULTS

Characterization of HTA$_{Sp}$. HTA$_{Sp}$ expressed in *E. coli* BL21 (DE3) cells yielded 16 mg of enzyme from 1 L of cell culture. The steady-state kinetic parameters of HTA$_{Sp}$-catalyzed acetylation of Hse were determined and are summarized in Table 1.

Double-reciprocal plots of the initial velocity patterns obtained from varying the concentrations of substrates reveal parallel lines (Figure 1). This result is consistent with the acetylation of L-Hse via a double-displacement or ping-pong mechanism.

To further support that HTA$_{Sp}$ catalyzes the acetyl transfer reaction via a double-displacement mechanism, we incubated the enzyme with ^{14}C-acetylCoA and monitored the transfer of the label to HTA$_{Sp}$ (Figure 2). The acetyl−enzyme complex collapses with the addition of L-Hse, consistent with the transfer of the radioactive group to the amino acid. The stoichiometry of acetylation was estimated to be ~14% after the excision of the labeled protein from the SDS−polyacrylamide gel, followed by scintillation counting. This value reflects the hydrolytic liability of the complex under these conditions.

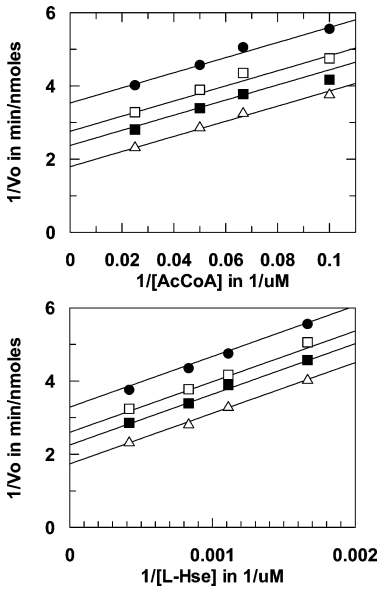

FIGURE 1: Double-reciprocal plots of the initial velocity patterns of HTA$_{Sp}$. (A) Varying concentrations of acetylCoA at a fixed L-Hse concentration (●, 600 μM; □, 900 μM; ■, 1200 μM; △, 2400 μM). (B) Varying concentrations of L-Hse at a fixed acetylCoA concentration (●, 10 μM; □, 15 μM; ■, 20 μM; △, 40 μM).

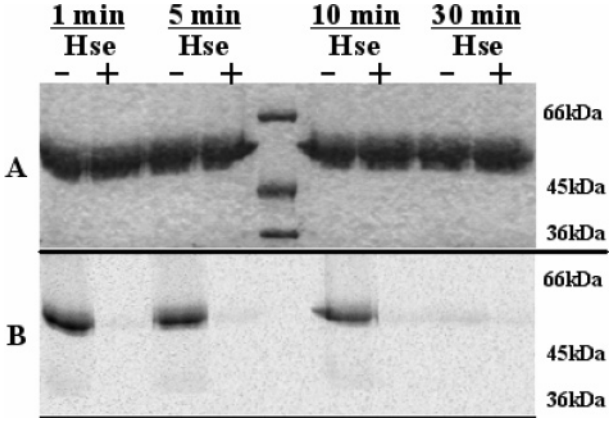

FIGURE 2: Identification of an acetylated HTA_{Sp} as an intermediate in L-Hse acetylation. ^{14}C-AcetylCoA was added to HTA_{Sp}, and the transfer of the radioactive label was monitored over time. (A) Coomassie-stained 12% SDS−polyacrylamide gel of the HTA_{Sp} reaction with ^{14}C-acetylCoA before and after the addition of L-Hse. Reactions were stopped at different time points by the addition of SDS−polyacrylamide gel electrophoresis loading dye. (B) Phosphor image of the SDS−polyacrylamide gel.

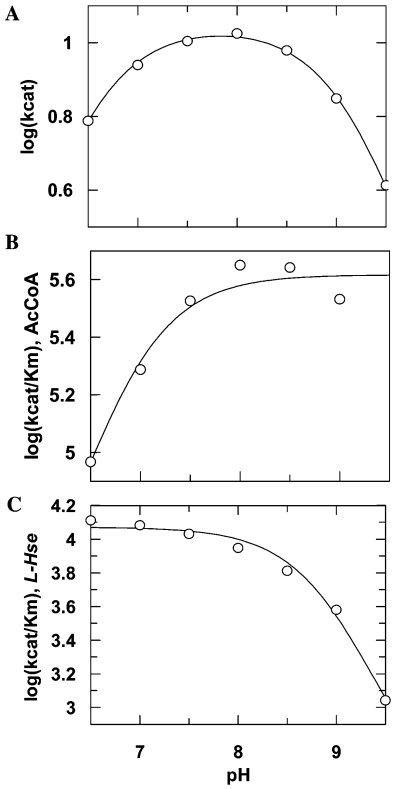

FIGURE 3: pH dependence of the kinetic parameters of HTA_{Sp} catalysis of L-Hse acetylation. (A) Dependence of k_{cat} on pH. (B) Dependence of $k_{cat}/K_{m\_acetylCoA}$ on pH. (C) Dependence of k_{cat}/K_{m_Hse} on pH.

pH Dependence of HTA_{Sp} Kinetic Parameters. The pH dependence of the kinetic parameters of HTA_{Sp} can reveal different ionization states of the enzyme and/or reactants that could affect the activity of the enzyme (*15*). The pH dependence of the steady-state rates of HTA_{Sp} was measured in the pH range of 6.5−9.5, and the data are summarized in Figure 3. The pH dependence of k_{cat} gives a bell-shaped curve indicating that, at both the low and high pH values, activity is affected with two pK_a values of 6.6 and 9.4 (Figure 3A). The effect on $k_{cat}/K_{m\_acetylCoA}$ is affected at the lower end of the pH range studied, with a single pK_a value of 6.4 (Figure 3B). Finally, the effect of pH on k_{cat}/K_{m_L-Hse} is only apparent at the higher end of the pH range, giving a slightly lower pK_a value of 9.4 (Figure 3C).

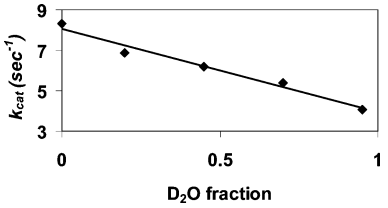

FIGURE 4: Proton inventory study of HTA_{Sp}. Effect of the fraction of D_2O (0, 20, 45, 70, and 95%) on the k_{cat} of HTA_{Sp} was determined and reveals a linear dependence.

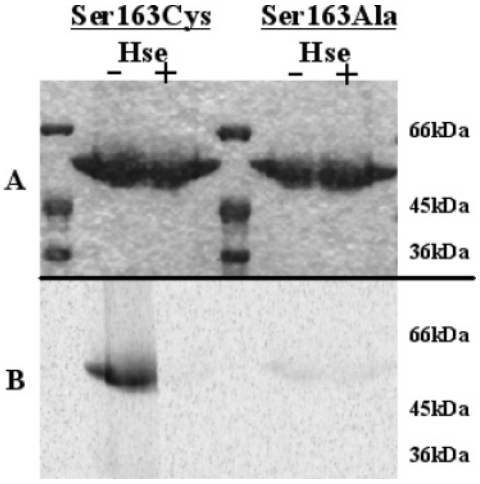

FIGURE 5: Identification of the ability of Ser163 site mutants to transfer the acetyl group of ^{14}C-acetylCoA via an acetyl−enzyme intermediate. (A) Coomassie-stained 12% SDS−polyacrylamide gel of Ser163Cys and Ser163Ala mutant reactions with ^{14}C-acetylCoA before and after the addition of L-Hse. Reactions were stopped after 30 min by the addition of SDS−polyacrylamide gel electrophoresis loading dye. (B) Phosphor image of the SDS−polyacrylamide gel.

Proton Inventory Experiments and Solvent Deuterium Isotope Effects. Solvent deuterium isotope effects of the forward reaction were determined by measuring the kinetic parameters in H_2O and 95% D_2O. When varying L-Hse, solvent isotope effects of 1.89 on k_{cat} and 2.03 on k_{cat}/K_{m_L-Hse} were obtained. When varying acetylCoA, solvent isotope effects of 1.96 on k_{cat} and 2.10 on $k_{cat}/K_{m\_acetylCoA}$ were obtained.

Proton inventory studies measured with increasing amounts of D_2O in the reaction mixture reveal a linear dependence with k_{cat} (Figure 4). These data are consistent with a single-proton transfer in the isotopically sensitive step (*16*).

Characterization of HTA_{Sp} Mutants. Analysis of HTA protein sequences reveals that these are members of the α/β-hydrolase fold superfamily, which are characterized by a catalytic triad with a nucleophilic residue in this motif, which is Ser, Cys, or Glu (*9*). Protein sequence alignments of HTAs reveal no consensus Cys, but there is an invariant Ser at position 163. Furthermore, our pH studies show dependence on a deprotonated amino acid with a pK_a value of 6.4−6.6, which could suggest the involvement of a His residue. Protein sequence alignment of HTAs reveals a single conserved His residue at position 432. There are several conserved Asp residues at positions 209, 374, and 403, which would complete the triad. Therefore, we constructed the mutants

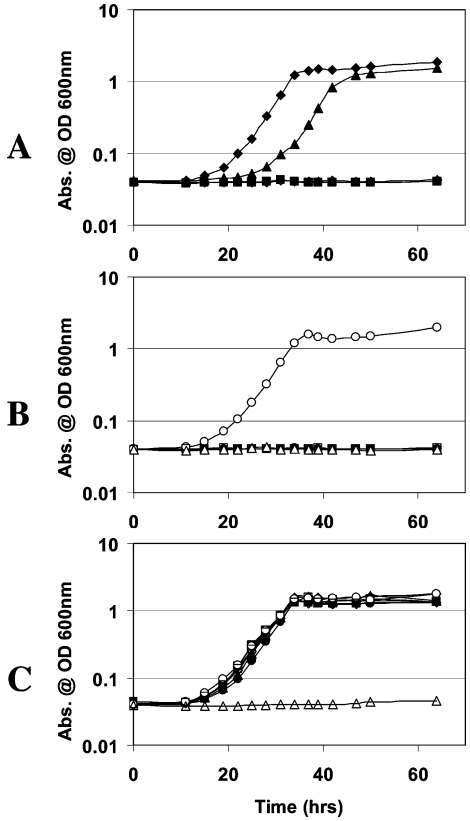

FIGURE 6: Growth curves of wild type and site mutants of HTA_{Sp} expressed in *S. cerevisiae* Δ*MET2* Met auxotroph in minimal media. (A) Growth of wild type (◆), Ser163Cys (▲), Ser163Ala (■), and His432Ala (◇) in minimal media lacking methionine. (B) Growth of Asp374Asn (○), Asp403Asn (●), pGal-cflag vector (□), and no vector (△) in minimal media lacking Met. (C) Growth of all of the constructs in minimal media supplemented with methionine.

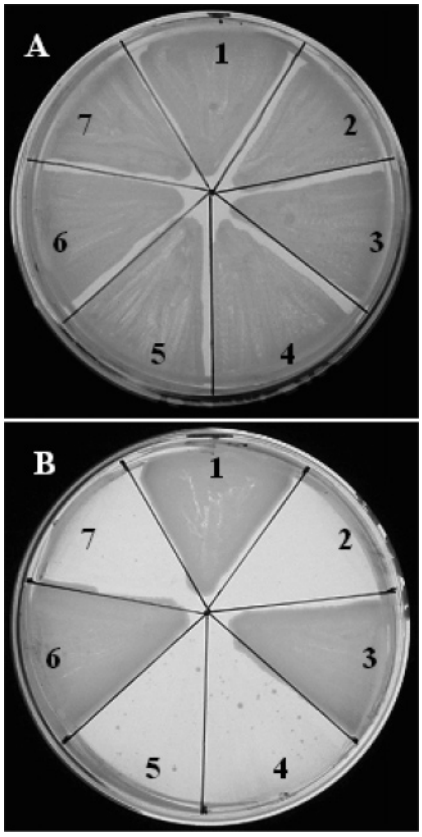

FIGURE 7: Wild type and mutants of HTA_{Sp} expressed in *S. cerevisiae* Δ*MET2* Met auxotroph on minimal media agar plates in the presence (A) and absence (B) of Met. 1, WT; 2, Ser163Ala; 3, Ser163Cys; 4, Asp403Asn; 5, His432Ala; 6, Asp374Asn; and 7, pGal-cFlag vector. Wild type, Asp374Asn, and Ser163Cys are capable of suppressing the Met auxotrophy.

Ser163Ala, Ser163Cys, Asp209Asn, Asp374Asn, Asp403Asn, and His432Ala, purified each, and studied their steady-state kinetic parameters (Table 1). The Ser163Ala, Asp403Asn, and His432Ala site mutants show no activity in our assay. These results are consistent with the identification of Ser163, Asp403, and His 432 as the catalytic triad residues.

We also monitored acetyl−enzyme intermediate formation using the site mutants to access the role of these mutants to catalyze the first half-reaction. Figure 5 reveals the ability of Ser163Cys to form an acetyl−enzyme intermediate, which breaks down after the addition of L-Hse. As expected, the Ser163Ala mutant could not form an acetyl−enzyme intermediate (Figure 5). His432Ala and Asp403Asn are weakly labeled when incubated with ^{14}C-acetylCoA (data not shown). The label is not released upon the addition of L-Hse to the reaction mixture or by the prolonged incubation time.

*Suppression of Δ*MET2* by HTA_{Sp} in S. cerevisiae.* Wild-type HTA_{Sp} and site mutants were expressed under the control of galactose induction in a *S. cerevisiae MET2* deletion strain. This mutant requires an exogenous amount of Met for growth in minimal media. The growth of this strain was assessed in broth and on agar plates of minimal media (YNB) in the presence and absence of Met, complimented by the wild type and the different site mutant alleles of HTA_{Sp} *in trans*. This experiment was designed to study the ability of HTA_{Sp} and its mutants to suppress Met auxotrophy because of the *MET2* gene disruption. In the presence of Met, all strains show similar growth to the wild type and reach saturation after 30 h (Figure 6A). When Met is absent, Asp374Asn and Ser163Cys were the only two mutants capable of reaching saturation levels of growth similar to the wild-type enzyme, although Ser163Cys is slower by 15 h (Figure 6B). These results were also confirmed on solid media, where the only strains capable of growing without Met have the wild-type, Asp374Asn, or Ser163Cys enzyme construct introduced *in trans* (Figure 7).

DISCUSSION

HTA is an essential enzyme required for the biosynthesis of Met from Asp. This enzyme catalyzes the transfer of an acetyl group from acetylCoA to the hydroxyl group of L-Hse, activating the terminal hydroxyl for eventual replacement by thiol to generate homocysteine, the penultimate step in Met biosynthesis (*17*). Blanchard's group has studied HTA from the bacterium *H. influenzae* and found that it operates by a ping-pong kinetic mechanism, forming an acetyl−enzyme intermediate before final transfer of the acyl group to L-Hse (*10*). Fungal HTAs share approximately 20% similarity with the bacterial enzymes and have an insert of approximately 100 amino acids located about 50 amino acids from the C terminus (Scheme 1). On the basis of these observations and the importance of this enzyme as a possible target for new antimicrobial agents, we have investigated the mechanism of HTA from the fission yeast *S. pombe* to establish if the fungal enzymes share overall mechanism with their bacterial counterparts and to identify important active-site residues involved in catalysis.

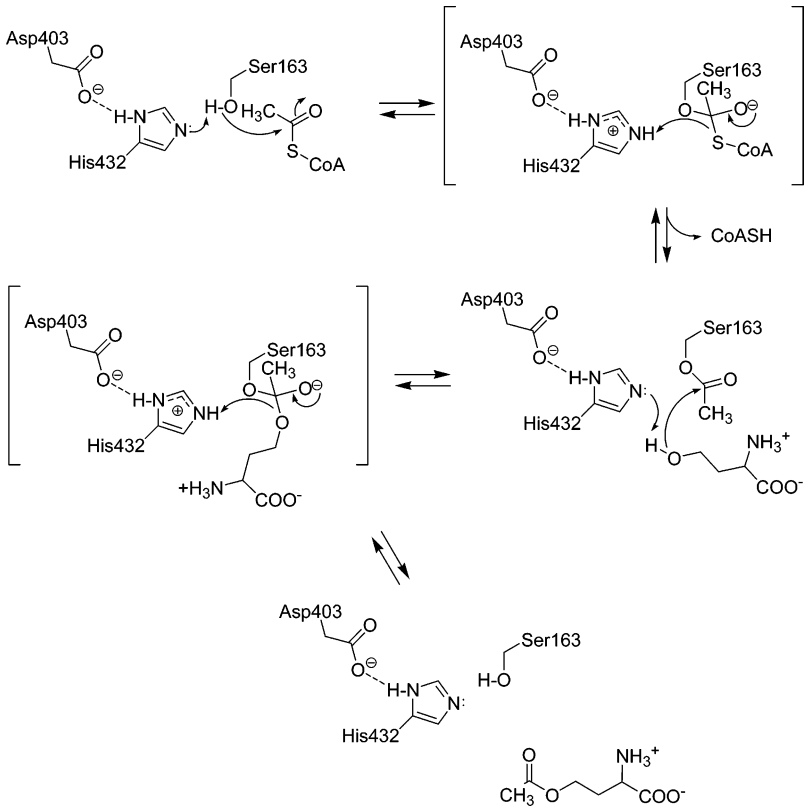

FIGURE 8: Proposed chemical mechanism of HTA_{Sp}. This enzyme uses a catalytic triad to transfer an acetyl group from acetylCoA to L-Hse via a ping-pong mechanism. The members of the catalytic triad are essential to facilitate this process by activating Ser163 for nucleophilic attack on the carbonyl center of acetylCoA. This triad is also likely important for activating the hydroxyl group of L-Hse for acetylation.

Analysis of steady-state kinetic parameters demonstrated that the acetylCoA Michaelis constant for the yeast enzyme is 4 times smaller than the *H. influenzae* enzyme (*10*), while the K_m for L-Hse is 8-fold higher. The catalytic constant (k_{cat}) is 10 times larger for the bacterial enzyme. The bacterial enzyme is therefore comparable with the fungal HTA in terms of acetylCoA capture (*18*) (k_{cat}/K_m on the order of 10^5 M^{-1} s^{-1}) but 80-fold less efficient at L-Hse capture in the steady state. These differences likely speak to the levels of intracellular substrate pools and the metabolic flux requirements within each organism.

While the fungal and bacterial HTAs differ in acylCoA K_m, they do share similar acylCoA specificity. Both fungal and bacterial enzymes show little differentiation between C2, C3, and C4 acylCoAs, with K_m values varying at most 2-fold. Therefore, HTAs likely share similar acylCoA-binding-site geometries.

HTA from *S. pombe* demonstrated parallel lines in Lineweaver−Burke plots of initial velocity studies, suggesting that HTA_{Sp} catalyzes the acetylation of L-Hse via a double-displacement (ping-pong) mechanism. This was supported by the capture of a labile acyl−enzyme intermediate when HTA_{Sp} was incubated with radiolabeled acetylCoA. The label was efficiently transferred to L-Hse, demonstrating competence in the second half-reaction of a double-displacement mechanism. These results were predicted given the precedent with the *H. influenzae* enzyme (*10*) and inclusion of HTA in the α/β-hydrolase fold enzyme superfamily that functions by nucleophilic catalysis (*9*). These enzymes frequently operate through a canonical catalytic triad, with nucleophilic residues partnered with 1−2 acid−base catalysts such as His and Asp.

Analysis of solvent isotope effects was consistent with rate-influencing proton transfer, and pH studies suggested participation of at least one base with pK_a 6.4−6.6, suggestive of His or possibly Asp/Glu. Amino acid sequence alignment of HTAs identified one conserved His, His432, and three conserved Asp in positions 209, 374, and 403. This alignment also identified a potential nucleophilic residue, Ser163. We mutated each of these residues and analyzed their impact on steady-state kinetics. The His432Ala and Asp403Asn mutants had no detectable activities implicating them in catalysis. Furthermore, Ser163Ala also had no detectable activity, while the Cys mutant was catalytically impaired but competent with roughly a 10-fold impact on k_{cat}/K_m for both acetylCoA and L-Hse substrates.

These results suggest a catalytic triad of Ser163, His432, and Asp403 participating in catalysis of Hse acetylation by HTA. A reasonable chemical mechanism is shown in Figure 8, where His432 and Asp403 assist in activation of Ser163 for formation of the acyl−enzyme. We speculate that these residues may also be involved in deprotonation of the second substrate Hse as shown in the figure. The *in vitro* results were recapitulated *in vivo* in an *S. cerevisiae MET2* null genetic background. Only the wild-type, Asp374Asn, and Ser163Cys enzymes could suppress Met auxotrophy. These results not only support the roles of Ser163, His432, and Asp403 in HTA function, but they also demonstrate that impairment of HTA activity is antifungal under Met limiting conditions.

Several studies have indicated the importance of the Asp pathway for the survival of microbes. A number of enzymes in this pathway have been validated as novel antimicrobial targets (*2*, *5*, *19*, *20*), and our results on HTA implicate it as

an essential enzyme for organisms in environments that are poor in Met concentrations such as serum [Met concentration of 20 μM (*21*)]. HTA is unique to fungi, Gram-positive, and some Gram-negative bacteria, and therefore, this enzyme presents the antimicrobial industry with a novel target. The double-displacement mechanism utilized by HTA_{Sp} via the Ser163 nucleophile also provides a unique anchor for inhibitor discovery. Drugs such as the β-lactams of the penicillin and cephalosporin class have been developed that alkylate the Ser nucleophilic residues of peptidoglycan transpeptidases, providing precedent for successful inhibition of therapeutically important enzymes. A similar strategy targeting HTA could generate novel antimicrobial agents, which are sorely needed in the face of drug resistance and the emergence of new pathogens.

NOTE ADDED AFTER ASAP PUBLICATION

This paper was published ASAP 09/24/05. The units for k_{cat}/K_m in the first paragraph under Figure 8 are now correct. The corrected version was published 09/29/05.

SUPPORTING INFORMATION AVAILABLE

Table listing oligonucleotide sequences used for gene amplification. This material is available free of charge via the Internet at http://pubs.acs.org.

REFERENCES

1. Umbarger, H. E. (1978) Amino acid biosynthesis and its regulation, *Annu. Rev. Biochem. 47*, 532−606.
2. Yang, Z., Pascon, R. C., Alspaugh, A., Cox, G. M., and McCusker, J. H. (2002) Molecular and genetic analysis of the *Cryptococcus neoformans* MET3 gene and a *met3* mutant, *Microbiology 148*, 2617−2625.
3. Huisman, G. W., and Kolter, R. (1994) Sensing starvation: A homoserine lactone-dependent signaling pathway in *Escherichia coli*, *Science 265*, 537−539.
4. Parsek, M. R., Val, D. L., Hanzelka, B. L., Cronan, J. E., Jr., and Greenberg, E. P. (1999) Acyl homoserine-lactone quorum-sensing signal generation, *Proc. Natl. Acad. Sci. U.S.A. 96*, 4360−4365.
5. Yamaguchi, H., Uchida, K., Hiratani, T., Nagate, T., Watanabe, N., and Omura, S. (1988) RI-331, a new antifungal antibiotic, *Ann. N. Y. Acad. Sci. 544*, 188−190.
6. Yamaki, H., Yamaguchi, M., Imamura, H., Suzuki, H., Nishimura, T., Saito, H., and Yamaguchi, H. (1990) The mechanism of antifungal action of (*S*)-2-amino-4-oxo-5-hydroxypentanoic acid, RI-331: The inhibition of homoserine dehydrogenase in *Saccharomyces cerevisiae*, *Biochem. Biophys. Res. Commun. 168*, 837−843.
7. Jacques, S. L., Mirza, I. A., Ejim, L., Koteva, K., Hughes, D. W., Green, K., Kinach, R., Honek, J. F., Lai, H. K., Berghuis, A. M., and Wright, G. D. (2003) Enzyme-assisted suicide: Molecular basis for the antifungal activity of 5-hydroxy-4-oxonorvaline by potent inhibition of homoserine dehydrogenase, *Chem. Biol. 10*, 989−995.
8. Rowbury, R. J., and Woods, D. D. (1964) *O*-Succinylhomoserine as an intermediate in the synthesis of cystathionine by *Escherichia coli*, *J. Gen. Microbiol. 36*, 341−358.
9. Ollis, D. L., Cheah, E., Cygler, M., Dijkstra, B., Frolow, F., Franken, S. M., Harel, M., Remington, S. J., Silman, I., and Schrag, J. (1992) The α/β hydrolase fold, *Protein Eng. 5*, 197−211.
10. Born, T. L., Franklin, M., and Blanchard, J. S. (2000) Enzyme-catalyzed acylation of homoserine: Mechanistic characterization of the *Haemophilus influenzae met2*-encoded homoserine transacetylase, *Biochemistry 39*, 8556−8564.
11. Leatherbarrow, R. J. (2000) *Grafit Ver 4*, Erithacus Software, Staines, U.K.
12. Higuchi, R., Krummel, B., and Saiki, R. K. (1988) A general method of *in vitro* preparation and specific mutagenesis of DNA fragments: Study of protein and DNA interactions, *Nucleic Acids Res. 16*, 7351−7367.
13. Ho, Y., Gruhler, A., Heilbut, A., Bader, G. D., Moore, L., Adams, S. L., Millar, A., Taylor, P., Bennett, K., Boutilier, K., Yang, L., Wolting, C., Donaldson, I., Schandorff, S., Shewnarane, J., Vo, M., Taggart, J., Goudreault, M., Muskat, B., Alfarano, C., Dewar, D., Lin, Z., Michalickova, K., Willems, A. R., Sassi, H., Nielsen, P. A., Rasmussen, K. J., Andersen, J. R., Johansen, L. E., Hansen, L. H., Jespersen, H., Podtelejnikov, A., Nielsen, E., Crawford, J., Poulsen, V., Sorensen, B. D., Matthiesen, J., Hendrickson, R. C., Gleeson, F., Pawson, T., Moran, M. F., Durocher, D., Mann, M., Hogue, C. W., Figeys, D., and Tyers, M. (2002) Systematic identification of protein complexes in *Saccharomyces cerevisiae* by mass spectrometry, *Nature 415*, 180−183.
14. Elble, R. (1992) A simple and efficient procedure for transformation of yeasts, *BioTechniques 13*, 18−20.
15. Fersht, A. (1985) in *Enzyme Structure and Mechanism*, pp 155−175, W. H. Freeman and Company, New York.
16. Quinn, D. M., and Sutton, L. D. (1991) in *Enzyme Mechanism from Isotope Effects*, pp 73−126, CRC Press, Inc., Boca Raton, FL.
17. Yamagata, S. (1987) Partial purification and some properties of homoserine *O*-acetyltransferase of a methionine auxotroph of *Saccharomyces cerevisiae*, *J. Bacteriol. 169*, 3458−3463.
18. Northrop, D. B. (1998) On the meaning of K_m and V_{max}/K_m in enzyme kinetics, *J. Chem. Educ. 75*, 1153−1157.
19. Ejim, L., Mirza, I. A., Capone, C., Nazi, I., Jenkins, S., Chee, G. L., Berghuis, A. M., and Wright, G. D. (2004) New phenolic inhibitors of yeast homoserine dehydrogenase, *Bioorg. Med. Chem. 12*, 3825−3830.
20. Pascon, R. C., Ganous, T. M., Kingsbury, J. M., Cox, G. M., and McCusker, J. H. (2004) *Cryptococcus neoformans* methionine synthase: Expression analysis and requirement for virulence, *Microbiology 150*, 3013−3023.
21. Fasman, G. D. (1976) *Handbook of Biochemistry and Molecular Biology*, 3rd ed., CRC Press, Cleveland, OH.

BI0514764